Chapter 19
Forecasting the Coastal Optical Properties Using Satellite Ocean Color

Robert Arnone, Brandon Casey, Sherwin Ladner, and Dong-Shang Ko

19.1 Introduction

Algorithms for ocean color bio-optical properties from space have advanced significantly in the last 20 years. Improved alogorithms have advanced beyond chlorophyll to characterize coastal optical properties such as absorption from phytoplankton, colored dissolved organic matter and detritus, in addition to backscattering from the particle distribution. These properties have provided new insights into the changing conditions along our coast. However, for many coastal management applications these satellite derived properties are insufficient to make real-time decisons (Arnone and Parsons, 2004). Daily satellite ocean color imagery represents a nowcast of bio-optical conditions. Although these near real-time bio-optical products can be made available within hours of a satellite over pass, they may be inadequate for operations. In the coastal waters, changes are occuring within hours as a result of the tidal fluxuations, river discharges, precipation, and local wind events so that the nowcast of the bio-optical properties may not be representative of local conditions within the 24 h period. Real-time coastal decisons on processes such as:

- dissipation of a coastal plume,
- movement of a Harmful Algal Bloom,
- river plume dispersion,
- turbidity frontal movement,
- chlorophyll bloom dispersion,
- larval fish migration,

all may require hourly forecast of bio-optical properties on a daily basis.

A sensible forecast of bio-optical properties along coastal waters requires an initialization field. This field can be best represented by the nowcast from ocean color bio-optical properties. Forecast and prediction of these properties can be defined

R. Arnone (✉)
Oceanography Division, Naval Research Laboratory, Stennis Space Center, MS 39529, USA
e-mail: arnone@nrlssc.navy.mil

V. Barale et al. (eds.), *Oceanography from Space*,
DOI 10.1007/978-90-481-8681-5_19,

by coupling these properties with a forecast circulation model. Circulation models have advanced significantly in the last 10 years and are approaching the confidence of weather forecasting. Circulation models are driven by winds and boundary conditions and are data assimilative of sea surface temperatures and sea surface height.

A major forcing in coastal enviroments is the result of the physical processes such as tides and winds and river discharge (Arnone et al., 2007). These physical processes change on scales of hours and results in advection of water masses. Although bio-optical processes are different than physical processes, we argue that bio-optical time scales occur on longer (on order of several days) compared to hourly time scales of the physical forcing (Stramska et al., 1995). The coupling of the bio-optical properties with the physical circulation models should provide a capability to forecast bio-optical properties on short times scales (days), where as at longer times scales (several days to weeks) the bio-optical processes may be decoupled from physical processes. For these longer time scale forecasting, other more complex bio-optical models may be required (Jolliff et al., 2008).

Satellite ocean color products are available from several satellites such that daily imagery is available along most coastlines. The initialization field of the coastal environment can be reinitialized daily using updated satellite bio-optical products such that a 24 h forecast should be possible for coastal decisons.

Our objective is to demonstrate the ability to derive bio-optical products along coastal waters on short time scales based on coupling ocean color bio-optical products with forecast ocean circulation models. We evaluate the bio-optical forecast using satellite imagery to determine an effective forecast probability.

19.2 Satellite Ocean Color and Circulation Models

Ocean color imagery from MODIS-Aqua was used to determine the bio-optical properties along the coast of northern Gulf of Mexico at the Mississippi River delta, USA for a month period in October, 2009. The Quasi Analytical Algorithm (QAA) (Lee et al., 2002; Martinolich, 2006) was used to process the imagery into backscattering (551) and absorption (443) and chlorophyll products. We used the 1 km products in our example, although new algorithms have been developed to determine these properties at 250 m (Ladner et al., 2007) which show improved capability for coastal management requiring the high resolution. The backscattering coefficient has been used to estimate an effective particle concentration, if we assume a specific size and composition and this property can be treated as a water mass tracer only affected by particle settling. The total absorption properties are influenced by phytoplankton, detritus and colored dissolved organic matter. The absorption properties are less of a conservative tracer since they are influenced by biological processes such as growth, decay photo-oxidation, etc. However, on these short time scales, we argue they also are minimal since diurnal changes in phytoplankton concentration can be small. This is especially appropriate in the coast

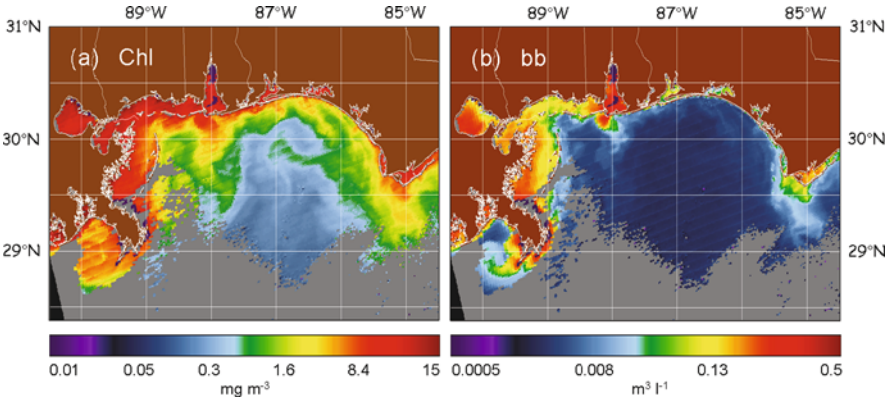

Fig. 19.1 MODIS derived coastal bio-optical properties of (**a**) chlorophyll [mg/m^3] and (**b**) backscattering (551) [m^3/l] from QAA, for 19 October 2009, along the Mississippi Delta USA. The clouds in the *lower part* of the images appear in *gray*

such as the Mississippi delta region which represents different bio-optical processes which include high sediment discharge from the river mouth, sediment resuspension along the coastal waters and offshore biological activity. We can examine the role of conservative and non-conservative processes within a 24 h forecast. Examples of the chlorophyll and backscattering a (551) are shown in Fig. 19.1 (panels a and b) for October 19, 2009.

The Navy Coastal Ocean Model (NCOM) was used to define the forecast circulation of the region. NCOM is a 41 layer model used for Navy operations. The model is forced with COAMPS winds and obtains boundary conditions from the "Global NCOM". This model assimilates both sea surface height fields from satellite altimeters and sea surface temperature from AVHRR (Martin, 2000). The model is run daily and reinitialized with updated winds fields and updated Sea Surface Height fields from satellite altimeters and Sea Surface Temperature. NCOM includes river discharge from 40 rivers entering the Gulf of Mexico. The nowcast and forecast out to 48 h is available from NCOM on a 3 h basis. Regional NCOM for the Intra-Americas Sea is the relocatable version of the NCOM. The horizontal current field (u, v) is required as an input to the bio-optical forecast. The expected format for these data files is NetCDF with one time step per file and u and v in separate files. The modeled current field for each time step is required to perform the advection.

If model fields are provided at a lower temporal resolution than the forecast, then an interpolation will be performed between each model time step, to produce the desired time steps. In the example shown in Fig. 19.2 (panel a), NCOM is at a resolution of 4 km and interpolated to 1 km, in order to match the satellite grid. NCOM has been shown to accurately represent the tides and circulation along the coast and will not be described in detail here (Ko et al., 2003).

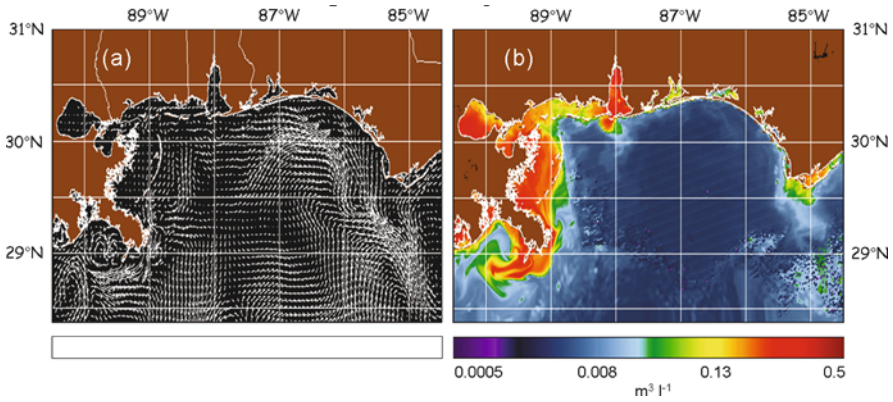

Fig. 19.2 *Panel* (**a**): NCOM surface currents of 19 October 2009. Currents are interpolated to the resolution of the imagery. *Panel* (**b**): initialization field of 19 October 2009 for backscattering coefficient. Notice the removal of the clouds using the steps outlined in the text

19.2.1 Bio-optical Initialization Field: "Nowcast"

The initialization bio-optical field is a critical step in the forecast. A bio-optical forecast requires complete spatial coverage in the initialization daily field. This is needed for several reasons: (1) to prevent gaps or No Data (ND) from creating artificial local boundary conditions in the advective forecast and (2) to prevent artificial bio-optical boundaries between ND and known data. The initialization field is constructed daily using all known data and the previous forecast field to provide a sensible bio-optical forecast. A realistic initialization field prevents abrupt data recreation and boundaries from artistically propagating into the forecast.

As seen in Fig. 19.1, a major limitation of the ocean color imagery is that complete coverage of bio-optical properties is not available daily. There are many times when limited coverage results from either cloud cover, algorithms failure (atmospheric, high turbidity, saturated radiance, etc.), no satellite coverage. These limitations require a procedure to "fill in the gaps". The initialization field is based on a series of additive steps to establish the "most recent" bio-optical coverage used to set the forecast.

The additive pixel procedure is used to determine the complete spatial distribution of coastal bio-optical properties. The hierarchy and details of the procedure are discussed in detail in Casey and Arnone (2007). The "gap filler" procedure is summarized in Steps 1–4:

1. today's bio-optical properties (best and most accurate);
2. spatial convolution of bio optical data in step 1 out several pixels (fills small holes, speckle, etc.);
3. triangular interpolation of data in Step 2 to fill in gaps;
4. yesterday's 24 h bio-optical forecast.

Depending on the area and cloud coverage, the bio-optical coverage takes about 1–2 weeks before a coherent bio-optical field initialization and forecast field can be established. Additionally, as increased satellite bio-optical data enters the initialization process, the bio-optical forecast improves, and it is then used in the next day's initialization field. This forecast "spin-up" time has been used in a variety of "cloudy" coastal regions with partial ocean coverage. A similar procedure to generate the initialization field is used in weather forecasting. The procedure has the advantage that for each day the "best" and most recent data enters the forecast. However, the entire bio-optical properties along a coast line can change from 1 day to the next, for example, if a "cloud free" scene enters the initialization field when the previous days initialization was based only on a forecast. Because the initialization is performed daily, reinitialization to observation conditions is rapid and the forecast improves. An example of the initialization field of backscattering is shown in Fig. 19.2 (panel b).

19.3 Forecasting Using Eulerian Advection

The forecasting of bio-optical properties is performed by applying a simple advection approach to satellite derived bio-optical products using the NCOM forecast circulation model in order to forecast the surface optical properties. As was described earlier, the theoretical basis for this, assumes bio-optical properties are controlled solely by the physical circulation within a 24 h cycle. The bio-optical processes such as phytoplankton growth and decay and CDOM production and oxidation are not considered and are remissive. Previous efforts used a Lagrangian advection approach; however, this process was shown to produce significant errors along coastal boundaries in addition to the high computing requirements. For these reasons we switched to an eulerian approach (Arnone et al., 2006).

The NCOM model and the satellite derived bio-optical initialization field pixel grid are established based on the grid resolution of the image (in this case 1 km). The vertical fluxes into and out of the grid cells of the bio-optical properties are estimated from the horizontal fields. We apply a "thin-layer approximation" to extend surface 2D advection to 3 dimensions. The advection is performed on a surface layer, for convenience, at 1 m thickness, which goes up and down with free sea surface such that the vertical velocity is 0 at the surface. The vertical velocity at the base of the layer can be determined from divergence/convergence of horizontal currents following the volume conservation. The vertical flux is estimated assuming a uniform concentration of field at vertical. Forward time stepping with first-order upwind advection is applied to the vertical advection. For the horizontal advection of the satellite field, a third-order upwind advection scheme with flow adjustment is applied to reduce diffusion and to prevent "a numerical overshoot".

So, e.g., as the surface layer bio-optical properties move offshore and diverge from coastal boundaries, the vertical flux replenishes the bio-optical concentration from a vertical upwelling (flux) of the subsurface bio-optical property. Similarly, the vertical flux of bio-optical concentration can account for downwelling flux into

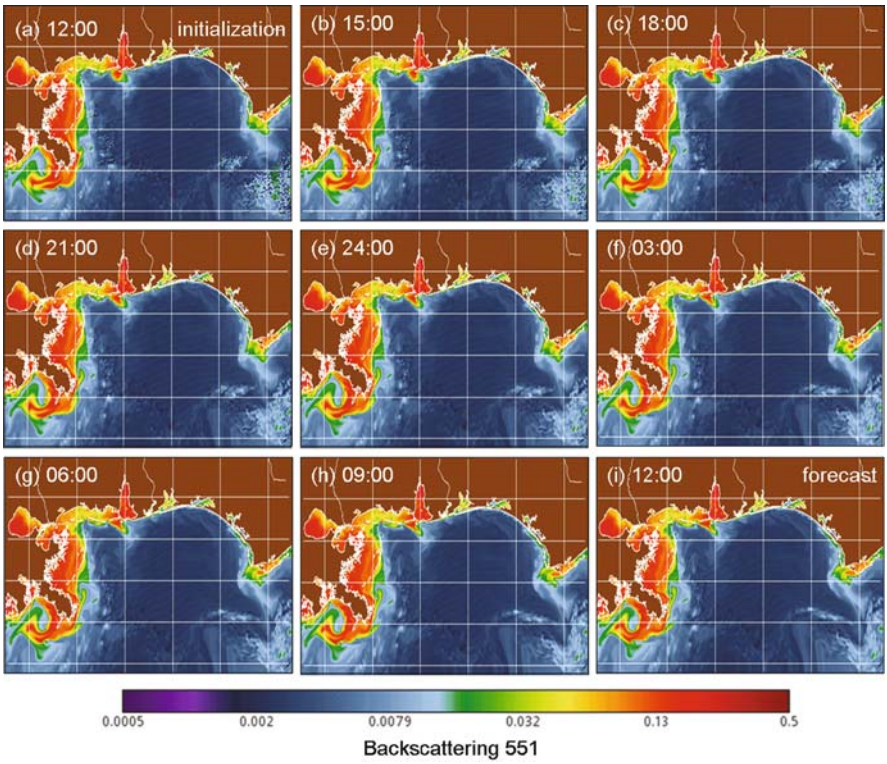

Fig. 19.3 Forecast of the surface backscattering coefficient for 19 October 2009, at 3 h intervals for 24 h. Time of the MODIS overpass was ~12:00 local. The various fileds show (**a**) 12:00 local (initialization), (**b**) 15:00 local, (**c**) 18:00 local, (**d**) 21:00 local; next day, (**e**) 24:00 local, (**f**) 03:00 local, (**g**) 06:00 local, (**h**) 09:00 local; (**i**) 12:00 local (24 h forecast)

the subsurface layers. However, these processes are not associated with bio-optical processes but are simply a conservative tracer of the bio-optical concentration physical flux.

The initialization field of backscattering (551) for October 19, 2009, was advected on an hourly basis and the surface bio-optical forecast is shown in Fig. 19.3 (panels a–j). This sequence represents the forecast of the surface bio-optical properties for every 3 h out to 24 h; i.e. next day. The initial field is created for approximately 11 AM local at the time of MODIS Aqua overpass and forecast out to 11 AM the next day.

19.4 Validation of the Bio-optical Forecast

The validation and estimate of the uncertainty in the bio-optical forecast can be quickly assessed by a pixel-by-pixel comparison of the 24 h forecast with the next day satellite bio-optical product. This is assuming that the next day bio-optical

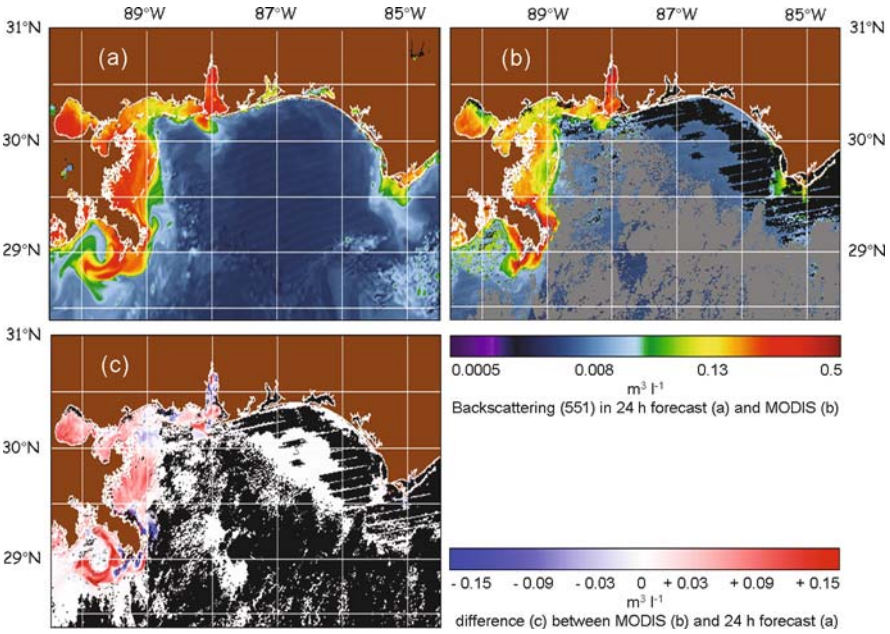

Fig. 19.4 Comparison and validation of forecast backscattering (551) for Oct 20, 2009: (**a**) 24 h forecast; (**b**) MODIS 20 October 2009, including clouds and atmospheric failures; (**c**) difference between MODIS and 24 h forecast (**b**–**a**), for *valid* retrievals only. Note the color coding in (**c**): *white* represents zero difference, *red* overestimated values, *blue* underestimated values. *Black* pixels are ND or clouds

property of interest can be retrieved (i.e. cloud free field). Satellite retrieved bio-optical properties are assumed valid. We assess the forecast accuracy based on a match up with these values. A difference comparison is computed only at locations where satellite retrieved properties occur (i.e. we do not use "gap filled"-derived bio-optical properties, described earlier in the validation procedure).

The difference between the backscattering forecast and next day's image indicates both over-estimating and under-estimating of the backscattering coefficient. We call this difference the "forecast error". In the example shown in Fig. 19.4, we notice that the Mississipi river plume was forecast to be advected to the west more so than what was observed in the next day's image. The difference image (Fig. 19.4c) shows higher backscattering (color coded red) than observed to the west of the river plume.

The satellite images of bio-optical properties provide an input into both the "now-cast" or initialization field and the validation field. Notice that the forecast error, (i.e. over or under estimated values) are spatially distributed and that certain regions have greater differences than others. These differences, however, are for an individual day's forecast and evaluation of a forecast is typically based on the forecast performance over a longer time sequence. As in weather predictions, a statistical approach to forecasting is used for an evaluation.

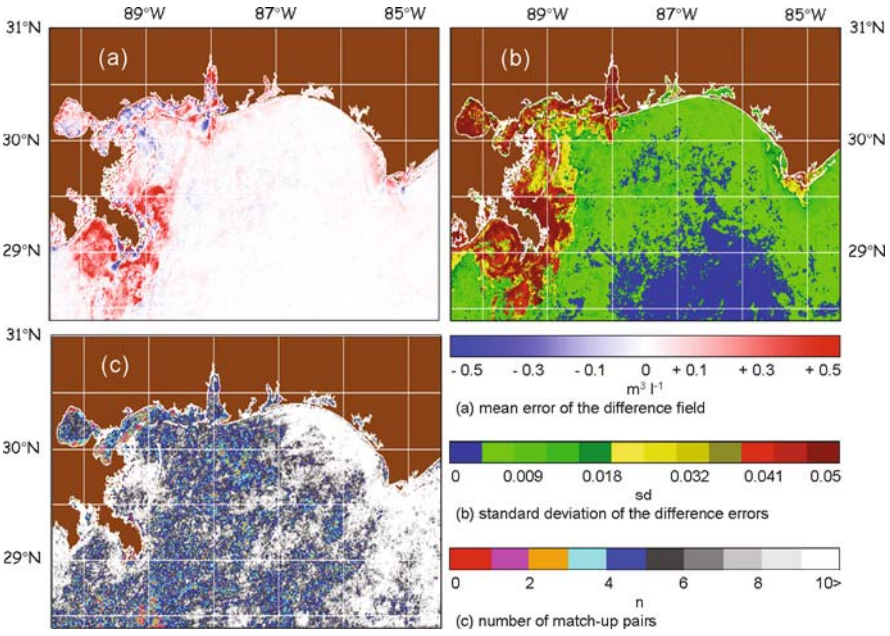

Fig. 19.5 Backscattering forecast error for month of October 2009 (~30 day): (**a**) mean error of the difference field; (**b**) standard deviation of the difference errors, (**c**) number of match-up pairs where the differences were computed (1–10+ days) in the month

The validation procedure described for computing the "forecast error" – which includes: (a) developing a daily initialization field, (b) 24 h forecast of the backscattering coefficient and (c) the comparison with the next day's image – was run for a 31 day sequence from October 1 to October 31, 2009. As expected, the daily forecast error was seen to change spatially. Certain regions showed more skill in bio-optical forecast than others. To assess this regional forecast skill, we determined the mean error of the difference field for the backscattering coefficient between the forecast and the next day's image (Fig. 19.5). The mean error field for this monthly period identifies the locations of higher and lower uncertainty of the forecast (Fig. 19.5a). White areas represent zero difference, red overesimated error and blue underestimated error. Note the overestimates in the location of the Mississipi river plume. There are regions where both over- and under-estimates of the forecast error occur on a monthly basis. However these errors are not clearly represented just by the monthly mean difference – i.e. positive and negative means can result in zero mean (white area).

To address these forecast errors, one must consider the standard deviation (sd) of the difference field (Fig. 19.5b). The standard deviation of this field illustrates the error about the mean and is perhaps a better way to represent forecast error. Along dynamic frontal locations, where both over- and under-estimates of the backscattering occur during the month, in response to the errors due to frontal movements, e.g.,

there will be a high standard deviation compared to the low mean error. Significant standard deviation errors (darker red) are observed in coastal areas associated with strong tidal regimes and the dissipation of the Mississippi River plume.

However, the total number of points used to determine the mean and standard deviation is critical to determine statistical validity. The number of matchup's pairs used to compute the mean and standard deviation for the month is represented in Fig. 19.5c at each location. This number represents the number of times during the month that a difference between the forecast field and a satellite retrieved backscattering product was computed. The greater number of matchup pairs, i.e. >10+ (color coded in white), represents valid statistical relationships,compared to the low numbers such as 4 and 5 (color coded in light and dark blue).

Notice that in areas where there are high number of data pairs (white in Fig. 19.5c), the monthly mean forecast errors are low (white in Fig. 19.5a) especially in the western region. The Mississippi River plume statistics are mixed. Representative errors occur where there are high numbers (white in Fig. 19.5c) in addition to a high mean error (red or blue in Fig. 19.5a). In the areas where there are lower number of match ups (light or dark blue in Fig. 19.5c) and the forecast error is high (red in Fig. 19.5a) the forecast errors are not representative. At these locations where the numbers are low, the statistical forecast error is unreliable.

In order to determine how the forecast of the backscattering compares with monthly "climatology", we examined the monthly mean and standard deviation of the backscattering coefficient for October 2009, which was computed based only on satellite derived backscattering (Fig. 19.6). As expected, the mean backscattering distributions do not show the small scale plumes and eddies along the coast as observed in October 19, and in the optical forecast. The monthly mean distribution is much different from the individual day's imagery and the forecast. The monthly standard deviation of backscattering (Fig. 19.6b) represents substantial changes in coastal backscattering which we believe is primarily resulting from the monthly

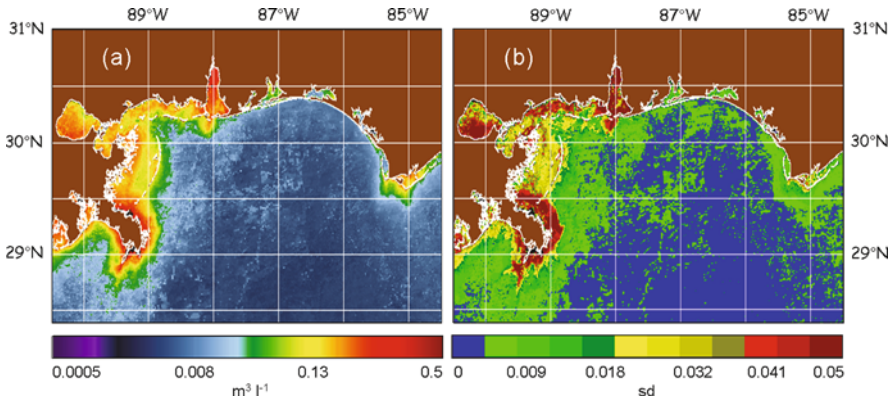

Fig 19.6 Monthly October 2009 backscattering (551) coefficient derived from MODIS –Aqua: (**a**) monthly mean and (**b**) standard deviation from the mean

variability in the physical processes and secondarily to the monthly bio-optical processes. Notice that regions with the highest standard deviation of backscattering (Fig. 19.6b) are locations associated with physical forcing in strong tidal regimes and coastal plumes.

We define the 24 h "persistence error" of the backscattering product as the difference within a 24 h change in backscattering. High changes indicate high persistence error, or lack of persistence. A lower error suggests that small changes occur and a similar backscattering coefficient can be used from 1 day to the next to represent the forecast. The persistence error is computed by differencing locations using two sequential (within 24 h) satellite backscattering fields.

The difference is computed daily and then averaged over the month. The persistence error represents change resulting from both physical and bio-optical processes, since it is based only on observed satellite retrievals of backscattering products and not on the physical circulation model. We computed this monthly persistence error field for October 2009, as mean and standard deviation (Fig. 19.7a, b).

To evaluate the representativeness of the monthly "persistence errors" of the mean and standard deviation, the number of match up samples (or satellite observed pairs) for each grid point is shown in Fig. 19.7c. This is the number of data points

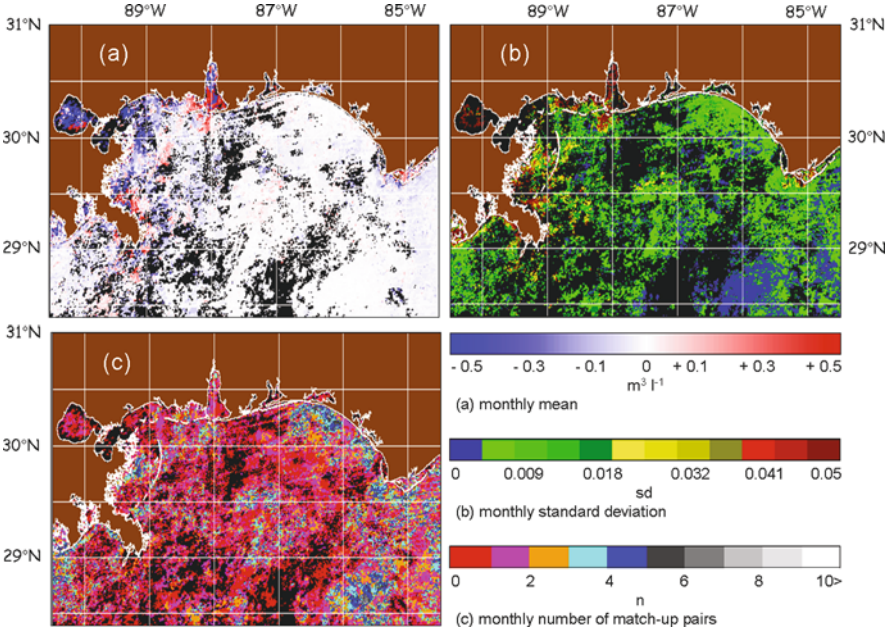

Fig. 19.7 The backscattering coefficient "persistence error" was computed as difference between two satellite backscattering retrievals within a 24 h period and statistics assembled for October 2009: (**a**) monthly mean (*black areas* indicate no pair of 24 h difference were observed); (**b**) monthly standard deviation; and (**c**) number of observational pairs used to generate the monthly statistics

used to compute the mean and requires two satellite products within 24 h. The large amount of black, red and pick (0,1,2) areas in Fig. 19.7c, indicate that there were few samples to compute the mean for the 31 day period and the mean and standard deviation persistence errors not representative. Therefore, the low persistence error observed (Fig. 19.7a) is misleading since there were very few points. A longer time period or more sequential observations is required to define the daily "persistence error"; although these statistics are difficult to obtain.

19.4.1 Persistence and the Forecast Error

The comparison between the persistence (Fig. 19.7) and forecast (Fig. 19.5) errors suggests persistence is better than forecast. However, several issues should be considered in these results. The number of samples used to compute persistence error (Fig. 19.7c) is small compared to those used for forecast error (Fig. 19.5c) because the calculation of the persistence error is dependent on cloud free "observations" from "two" sequential days, whereas forecast error is dependent on cloud free "observation" in one image. Although the persistence error has a lower mean and lower standard deviation than the forecast error, the small sample size in the persistence errors is not statistically valid and requires more data points.

Additionally, the forecast error was computed based on the initialization field which can include gap filled observations that were based on a previous forecast. For multiple cloudy or no observation days, the initialization field and the forecast would be based on old data that is greater than 24 h. This essentially assumes an older than 24 h observation used in the initialization field and the forecast error represents the error in many cases much greater than 24 h. Therefore, the forecast errors would be based on the age of the initialization field. This accounts for the higher error for the 24 h forecast (Fig. 19.5a). The advantage using the forecast error is that this statistics error is computed based on a much larger region and has a greater statistical number compared to the persistence error.

19.5 Uncertainty in the Forecast

We argued that for short time scales, the physical processes are responsible for controlling the distribution of surface bio-optical properties. Based on this, can we assess the uncertainty in the bio-optical forecast and determine where the error can occur? The first and perhaps largest uncertainty is from the physical circulation model. Although this model has been shown to represent the surface ocean conditions accurately, there is some temporal and spatial uncertainty of these processes which we did not represent. As discussed previously, the forecast physical models have several methods to assess their uncertainty which were not addressed here. A physical model can be set up to run with different initialization conditions which consider (1) grid resolution of the wind forcing fields (2) grid resolution of

the bathymetry (3) model grid spacing (4) vertical layer spacing (5) boundary conditions etc. The physical model can run a set of ensemble (typically ~40) to determine the uncertainty in the currents forecast field (Rixen et al., 2009). Using the current uncertainty, we can estimate the optical forecast for each of the ensemble currents and define the mean and spread of the optical forecast. We did not do this in these examples and assume the model currents were valid and correct. This is one source of optical forecast uncertainty that was not taken into account.

Satellite retrievals of the bio-optical properties (backscattering coefficient or chlorophyll) have an uncertainty based on the uncertainty of the algorithms. We implemented a set of uniform optical relationships that are used in the QAA algorithms which are considered standard. However, these relationships can change with location and bio-optical processes. The QAA algorithm has been shown to have some degree of uncertainty, (Lee et al., 2010) however these relationships should work well in the Gulf of Mexico. The uncertainty from these algorithms can influence the initialization and forecast. We assume the uncertainty of the algorithms is similar from 1 day's satellite image to another. Lastly, satellite retrievals require processing for atmospheric correction in addition to the in-water algorithms. The uncertainty in the aerosol models used for atmospheric correction is spatially and temporally changing, especially in coastal areas where aerosol optical depths are variable. We did not include this source of uncertainty of the atmospheric correction in the MODIS backscattering retrievals that were used in the forecast.

19.6 Conclusion

The retrievals of bio-optical properties from ocean color satellite have made significant advances in defining a "nowcast" of coastal conditions. New capability is required for coastal operations, coastal managers and researchers to forecast these properties on time scales of hours to weeks. The coastal environment changes on scales of hours, mostly as a result of the physical forcing associated with tidal, discharge and currents. We coupled daily surface ocean color properties of the backscattering coefficient at 551 nm and chlorophyll concentration to a physical circulation model and advected the field to determine an hourly forecast of the satellite derived properties.

The forecast of bio-optical properties is reinitialized daily as new satellite observations enter the forecast. The methods to construct a gap filled initialization field and integrate it into a coastal bio-optical forecast system required approximately 1–2 weeks spin-up time, and is based on availability of cloud free observations. We illustrate a 1 month daily forecast of the surface particle backscattering properties for October 2009.

A daily 24 h forecast of the backscattering coefficient was evaluated based on comparison with the "next day's" derived product. We conducted the validation and uncertainty of daily bio-optical forecast for a 1 month period to estimate spatial statistical relationships of the forecast uncertainty. The October 2009 statistics (mean

and standard deviation) of the backscattering coefficient forecast were characterized by the "forecast error", and "persistence error".

The forecast error showed higher errors in locations where there are strong currents and significant changes in the dynamics. We attributed these to uncertainty in the physical processes of the model forecast. The statistics of the persistence error (daily changes in satellite bio-optical properties), although appearing low, are not representative of the changing bio-optical conditions since the number of satellite observations used to generate the persistence statistics is not representative. We presented the forecast errors and persistence errors as absolute values. Perhaps a better way to describe the error would be using a percent difference in the forecast error. This may be more useful for managers using the forecast to look for maximum changes.

Coastal managers and researchers require new methods similar to weather forecasting to assess the coastal ecological conditions on time scale of hours. We demonstrated a new capability for using ocean color remote sensing to provide both the initialization and validation for bio-optical forecasting. On short time scales the physical processes are shown to be representative of the distributions of bio-optical properties. Future capabilities in ecological forecasting will rely on some degree of physical forcing in addition to bio-optical processes. We have shown an initial capability for coastal optical forecasting. However, improved methods to characterize the forecast uncertainty which are used in weather forecasting can be applied to bio-optical forecasting in the immediate future.

Acknowledgements This research was supported by the Naval Research Laboratory 6.1 "BIOSPACE "program and NASA REASoN program "Integrated analyses of ocean products in the Gulf of Mexico". Thanks to reviewers for useful suggestions and comments.

References

Arnone RA, Casey B, Ko DS, Flynn P, Carollo L, Ladner S (2007) Forecasting coastal optical properties using Ocean Color and coastal circulation models. SPIE Optics and Photonics, Conference 6680-43, San Diego, CA

Arnone RA, Flynn P, Ko DS, Martinolich P, Gould R, Haltrin V (2006) Forecasting optical properties from satellite derived optical properties. Proceedings of the Ocean Optics XVIII, Montreal, Canada

Arnone RA, Parsons AR (2004) Real-time use of ocean color remote sensing for coastal monitoring. In: Miller RL, Del Castillo CE, McKee BA (eds.) Remote sensing of the coastal environments, Chapter 14, Springer Publishing, Kluwer Academic, Dordrecht, pp. 317–337

Casey B, Arnone RA (2007) Simple and efficient technique for spatial and temporal composite imagery. SPIE Optics and Photonics, Conference 6680-43, San Diego, CA

Jolliff JK, Kindle J, Shulman I, Penta B, Friedrichs M, Helber R, Arnone RA (2008) Summary diagrams for coupled hydrodynamic – ecosystem model skill assessment. J Mar Sys 76(1–2):64–82

Ko DS, Preller RH, Martin PJ (2003) An Experimental Real time Intra Americas Sea Ocean Nowcast/Forecast System for Coastal Prediction. AMS 5th Conference on Coastal Atmospheric & Oceanic Prediction & Processes, New York

Ladner SD, Sandidge JC, Lyon PE, Arnone RA, Gould RW, Lee ZP, Martinolich PM (2007) Development of finer spatial resolution optical properties from MODIS. Proceedings, SPIE Optics and Photonics Meeting, San Diego, CA

Lee Z, Arnone R, Hu C,Werdell PJ, Lubac B (2010) Uncertainty of optical parameters and their propagations in an analytical ocean color inversion algorithm. Appl Opt 49(3):369–381

Lee Z, Carder KL, Arnone R (2002) Deriving inherent optical properties from water color: a multiband quasi-analytical algorithm for optically deep waters. Appl Opt 41(27):5755–5772

Martin PJ (2000) A description of the Navy Coastal Ocean Model, Version 1.0. NRL Report: NRL/FR/7322-009962. p. 39

Martinolich PM (2006) The Automated Satellite Data Processing System. NRL website, http://www7333.nrlssc.navy.mil/docs/aps_v4.0/user/aps/ version 4.0

Rixen M, Book JW, Carta A, Grandi V, Gualdesi L, Stoner R, Ranelli P, Cavanna A, Zanasca P, Baldasserini G, Trangeled C, Lewis C, Trees C, Grasso R, Giannechini S, Fabiani A, Merani D, Berni A, Leonard M, Paul Martin P, Rowley C, Hulbert M, Quaid A, Goode W, Preller R, Pinardi N, Oddo P, Guarnieri A, Chiggiato J, Carniel S, Russo A, Tudor M, Lenartz F, Vandenbulcke L (2009) Improved ocean prediction skill and reduced uncertainty in the coastal region from multi-model super-ensembles. J Mar Syst Coast Processes Chall Monit Prediction 78(S1):S282–S289

Stramska M, Dickey TD, Plueddemann A, Weller R, Langdon C, Marra J (1995) Bio-optical variability associated with phytoplankton dynamics in the North Atlantic ocean during spring and summer of 1991. J Geophys Res 100(C4):6621–6632